

Net reservoir discrimination through multi-attribute analysis at single sample scale

Jonathan Leal¹, Rafael Jerónimo¹, Fabian Rada^{2*}, Reinaldo Vilorio² and Rocky Roden³ present a new approach to net reservoir discrimination using multi-attribute seismic analysis at a single sample resolution, complemented by bivariate statistical analysis from petrophysical well logs.

Introduction

Self-Organizing Map (SOM) is an unsupervised neural network – a form of machine learning – that has been used in multi-attribute seismic analysis to extract more information from the seismic response than would be practical using only single attributes. The most common use is in automated facies mapping. It is expected that every neuron or group of neurons can be associated with a single depositional environment, the reservoir's lateral and vertical extension, porosity changes or fluid content (Marroquín et al., 2009). Of course, the SOM results must be calibrated with available well logs. In this paper, the authors generated petrophysical labels to apply statistical validation techniques between well logs and SOM results. Based on the application of PCA to a larger set of attributes, a smaller, distilled set of attributes were classified using the SOM process to identify lithological changes in the reservoir (Roden et al., 2015).

A bivariate statistical approach was then conducted to reveal the relationship between two categorical variables: the individual neurons comprising the SOM classification volume and Net Reservoir determined from petrophysical properties (percentage of occurrence of each neuron versus Net Reservoir).

The Chi-Square test compares the behaviour of the observed frequencies (Agresti, 2002) for each SOM neuron lithological contrast against the Net Reservoir variable (grouped in 'Net

Reservoir' and 'no reservoir' categories). Additional data analysis was conducted to determine which neurons responded to the presence of hydrocarbons using box plots showing Water Saturation, Clay Volume, and Effective Porosity as Net Pay indicators. The combination of these methods demonstrated an effective means of identifying the approximate region of the reservoir.

About the study area

The reservoir rock consists of sandstones from the Upper Miocene age in a slope fan environment. These sandstones correspond to channel facies, and slope lobes constituted mainly of quartz and potassium feldspars cemented in calcareous material of medium maturity. The submarine slope fans were deposited at the beginning of the deceleration of the relative sea-level fall, and consist of complex deposits associated with gravitational mass movements.

Stratigraphy and sedimentology

The stratigraphic chart comprises tertiary terrigenous rocks from Upper Miocene to Holocene. The litho-stratigraphic units are described in Table 1.

Figure 1 (left) shows the facies distribution map of the sequence, corresponding to the first platform-basin system

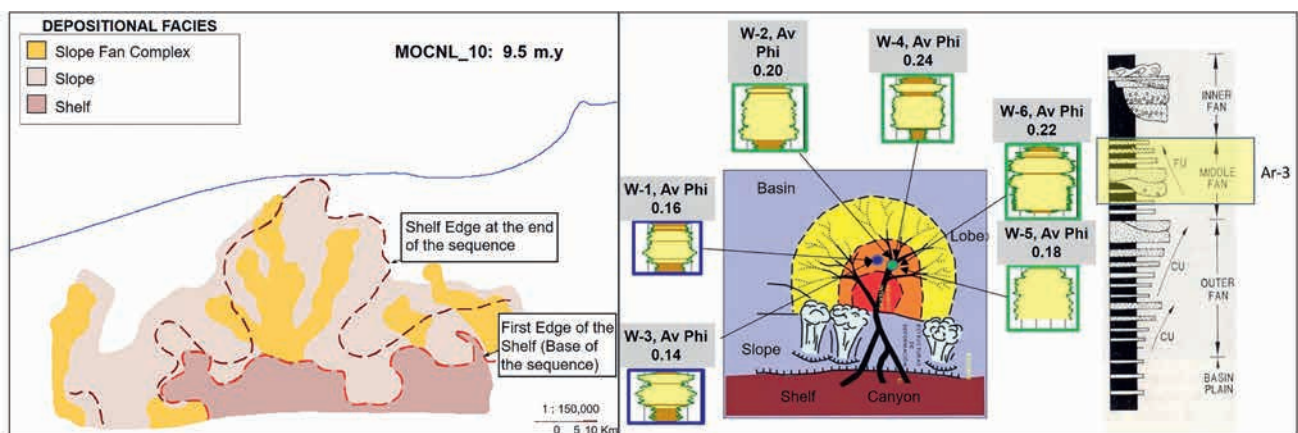


Figure 1 Left: Regional depositional facies. Right: Electrofacies and theoretical model, Muti (1978).

¹ PEMEX, Mexico | ² Oil and Gas Optimization SA de CV, Mexico | ³ Geophysical Insights, U.S.A.

* Corresponding author, E-mail: fabian.rada@ogopt.com

Stratigraphic Unit	Upper Miocene (target)	Lower Pliocene	Plio-Pleistocene	Undetermined
Lithology	Light grey sandstone / Dark grey shale in grayish green, sandy and slightly calcareous parts. Well classified.	Dark grey shale bodies in sandy, calcareous parts. Semi-consolidated small horizons of light gray sandstone	Light grey sand and light brown, semi-consolidated	Thick bodies of quartz sand of different shades, gray, amber and yellow. Intercalations of greenish grey and clear sandy gray shale
Matrix	Calcareous clay	Clayish	Calcareous clay	Clayish
Grain Size	Fine to medium and sub-rounded	Fine	Fine	Medium, angular gravel and mollusks.
Oil Impregnation	Light oil impregnation of yellow-cream fluorescence	Poor oil impregnation	Not reported	Not reported
Fossils	Not reported	Not reported	Some remains of mollus were observed	Shell fragments of mollus

Table 1 Stratigraphic Epoch Chart of study area

established in the region. The two dashed lines — one red and one dark brown — represent the platform edge at different times according to several regional integrated studies in the area. The predominant direction of contribution for studied Field W is south-north, which is consistent with the current regional sedimentary model. The field covers an area of approximately 46 km² and is located in facies of distributary channels northeast of the main channel. The reservoir is also well-classified and consolidated in clay matrix, and it is thought that this texture corresponds to the middle portion of the turbidite system. The observed electrofacies logs of the reservoir are box-shaped in wells W-2, W-4, W-5, and W-6 derived from gamma ray logs and associated with facies of distributary channels that exhibit the highest average porosity. In contrast, wells W-3 and W-1 are different — associated with lobular facies — according to gamma ray logs. In Figure 1 (right), a sedimentary scheme of submarine fans is proposed by Muti (1978).

Petrophysics

The Stieber model was used to classify Clay Volume (VCL). The Effective Porosity (PIGN) was obtained using the Neutron-Density model and non-clay water intergranular Water Saturation (SUWI) was determined to have a salinity of 45,000 ppm using the Simandoux model. Petrophysical cut-off values for effective porosity, water saturation, and clay volume were 0.10, 0.65 and 0.45, respectively.

Reservoir information

The reservoir rock corresponds to sands with Net Pay thickness ranging from 9 to 12 m, porosity between 18 and 25%, average permeability of 8-15 mD, and Water Saturation of approximately 25%. The initial pressure was 790 kg/cm² while the current pressure is 516 kg/cm². The main problem affecting productivity in this volumetric reservoir is pressure drop, being the mechanism of displacement the rock-fluid expansion, and gas in solution. Additionally, there are sanding problems and asphaltene precipitation.

Methodology

Multidisciplinary information was collected and validated to carry out seismic multi-attribute analysis. Static and dynamic

characterization studies were conducted in the study area, revealing the most relevant reservoir characteristics and yielding a better sense of the proposed drilling locations. At present, six wells have been drilled.

The original available seismic volume and associated gathers employed in the generation of multiple attributes and for simultaneous inversion were determined to be of adequate quality. At target depth, the dominant frequency approaches 14 Hz, and the interval velocity is close to 3300 m/s. Therefore, the vertical seismic resolution is 58 m. The production sand has an average thickness of 13 m, so it cannot be resolved with conventional seismic amplitude data.

Principal Component Analysis (PCA)

Principal Component Analysis (PCA) is one of the most common descriptive statistics procedures used to synthesize the information contained in a set of variables (volumes of seismic attributes) and to reduce the dimensionality of a problem. Applied to a collection of seismic attributes, PCA can be used to identify the seismic attributes that have made the greatest ‘contribution’, based on the extent of their relative variance to a region of interest. Attributes identified through the use of PCA are responsive to specific geological features, e.g., lithological contrast and fracture zones, among others. The output of PCA is an Eigen spectrum that quantifies the relative contribution or energy of each seismic attribute to the studied characteristic.

PCA applied for lithological contrast detection

The PCA process was applied to the following attributes to identify the most significant attributes to the region to detect lithological contrasts at the depth of interest: Thin Bed Indicator, Envelope, Instantaneous Frequency, Imaginary Part, Relative Acoustic Impedance, Sweetness, Amplitude, and Real Part.

Of the entire seismic volume, only the voxels in a time window (seismic samples) delimited by the horizon of interest were analysed, specifically 56 milliseconds above and 32 milliseconds below the horizon. The results are shown for each principal component. In this case, the criterion used for

the selected attributes were those whose maximum percentage contribution to the principle component was greater than or equal to 80%. Using this selection technique, the first five principal components were reviewed in the Eigen spectrum. In the end, six attributes of the first two principal components were selected (Figure 2).

Simultaneous classification of seismic attributes using a self-organizing map (SOM) neural network at voxel scale

The SOM method is an unsupervised, machine learning classification process where a neural network is trained from the input data alone. In this case, seismic data. The SOM process is an excellent, robust classification method in that it is non-linear and sensitive to subtle changes in the data. A SOM consists of components (vectors) called neurons or classes. Values in the data are compared employing neurons that detect and classify patterns in the seismic attribute volumes, typically multiple attribute volumes simultaneously. The SOM process, which is applied in Euclidian attribute space, is capable of detecting groupings of data through training and mapping. (Such groupings are a result of changes in the geology and stratigraphy within the volume; therefore the classification results indicate these changes.) The result of the SOM maps the neurons (classes) on to a two dimensional,

hexagonal or rectangular grid, sometimes referred to as Kohonen Map after Teuvo Kohonen who developed the method (Kohonen, 1982; Kohonen, 2001). In effect, the SOM process is a mechanism for dimensionality reduction, mapping a larger space to a smaller one. The procedure for locating a vector from the data space on the map is to find the neuron with the vector of weights (smaller Euclidian distance) closer to the vector of the data space, i.e., the ‘winning neuron.’ (The subject of this analysis accounted for seismic samples located within the time window covering several samples above and below the target horizon throughout the study area).

SOM classification for lithological contrast detection

The following six attributes were inputted to the SOM process with 25 classes (5 X 5) stipulated as the desired output: Envelope, Hilbert, Relative Acoustic Impedance, Sweetness, Amplitude, and Real Part.

As in the PCA analysis, the SOM was delimited to seismic samples (voxels) in a time window following the horizon of interest, specifically 56 milliseconds above to 32 milliseconds below. The resulting SOM classification volume was examined with several visualization and statistical analysis techniques to associate SOM classification patterns with reservoir rock.

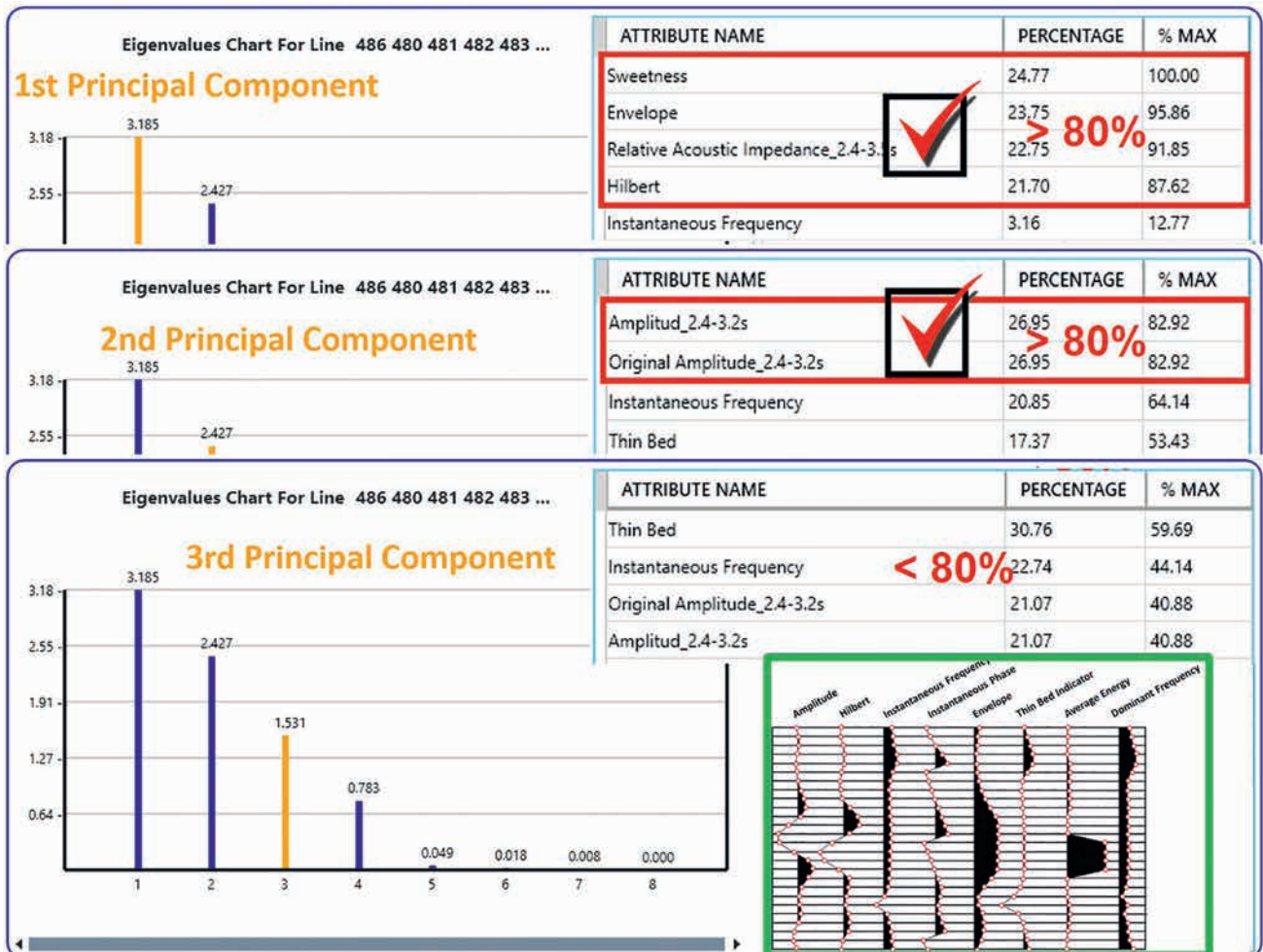


Figure 2 PCA results for lithological contrast detection.

3D and plan views

One way of identifying patterns or trends coherent with the sedimentary model of the area is visualizing all samples grouped by each neuron in 3D and plan views using the stratal-slicing technique throughout the reservoir. The Kohonen SOM and the 2D Colourmap in Figure 3 (lower right) ensures that the characteristics of neighbouring neurons are similar. The upper part of Figure 3 shows groupings classified by all 5x5 (25) neurons comprising the neural network, while in the lower part there are groupings interpreted to be associated with the reservoir classified by a few neurons that are consistent with the regional sedimentary model, i.e., neurons N12, N13, N16, N17, N22, and N23.

Vertical seismic section showing lithological contrast SOM

The observed lithology in the reservoir sand is predominantly made up of clay sandstone. A discrete log for Net Reservoir was generated to calibrate the results of the Lithological Contrast SOM, using cut-off values according to Clay Volume and Effective Porosity. Figure 4 shows the SOM classification of Lithological Contrast with available well data and plan view. The samples grouped by neurons N17, N21, and N22 match with Net Reservoir discrete logs. It is notable that only the well W-3 (minor producer) intersected the samples grouped by the neuron N17 (light blue). The rest of the wells only intersected neurons N21 and N22. It is important to note that these features are not observed on the conventional seismic amplitude data (wiggle traces).

Stratigraphic well section

A cross-section containing the wells (Figure 5) shows logs of Gamma Ray, Clay Volume, perforations, resistivity, Effective Porosity, Net Reservoir with lithological contrast SOM classification, and Net Pay.

The results of SOM were compared by observation with discrete well log data, relating specific neurons to the reservoir. At target zone depth, only the neurons N16, N17, N21, and N22 are present. It is noteworthy that only W-3 well (minor producer) intersect clusters formed by neuron N17 (light blue). The rest of the wells intersect neurons N16, N21, N22, and N23.

Statistical analysis Vertical Proportion Curve (VPC)

Traditionally, Vertical Proportion Curves (VPC) are qualitative and quantitative tools used by some sedimentologists to define succession, division, and variability of sedimentary sequences from well data, since logs describe vertical and lateral evolution of facies (Viloria et al., 2002). A VPC can be modelled as an accumulative histogram where the bars represent the facies proportion present at a given level in a stratigraphic unit. As part of the quality control and revision of the SOM classification volume for Lithological Contrasts, this statistical technique was used to identify whether in the stratigraphic unit or in the window of interest, a certain degree of succession and vertical distribution of specific neurons observed could be related to the reservoir.

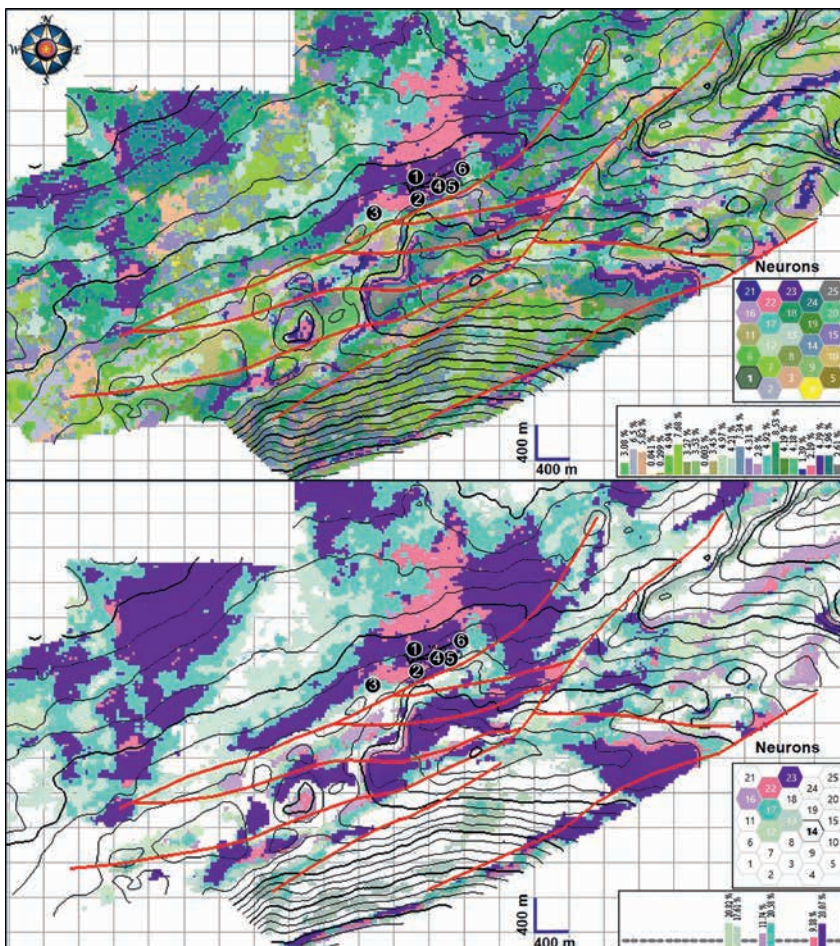


Figure 3 Plan view with geological significance preliminary geobodies from Lithological Contrast SOM. Below: only neurons associated with reservoir are shown.

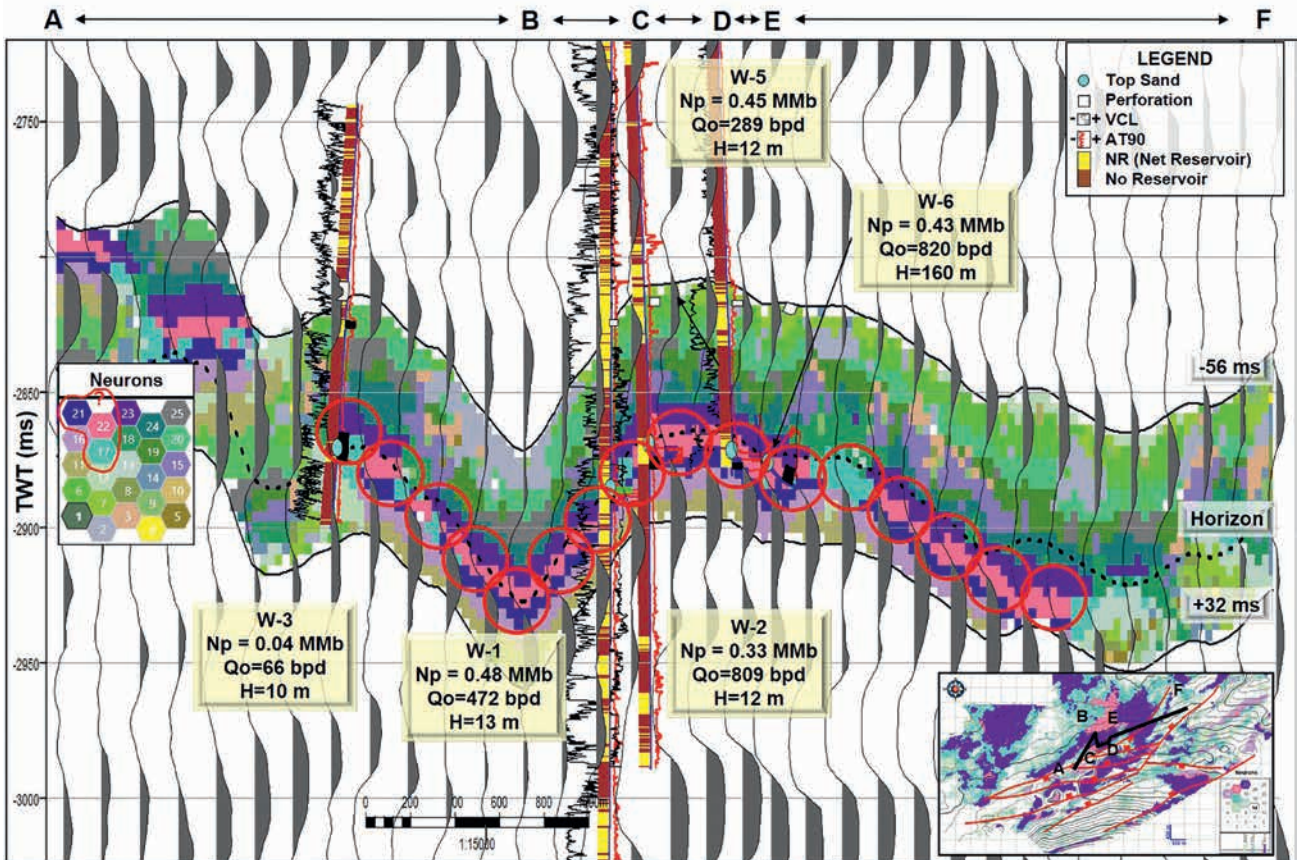


Figure 4 Vertical section composed by the SOM of Lithological Contrast, Amplitude attribute (wiggle), and Net Reservoir discrete property along wells.

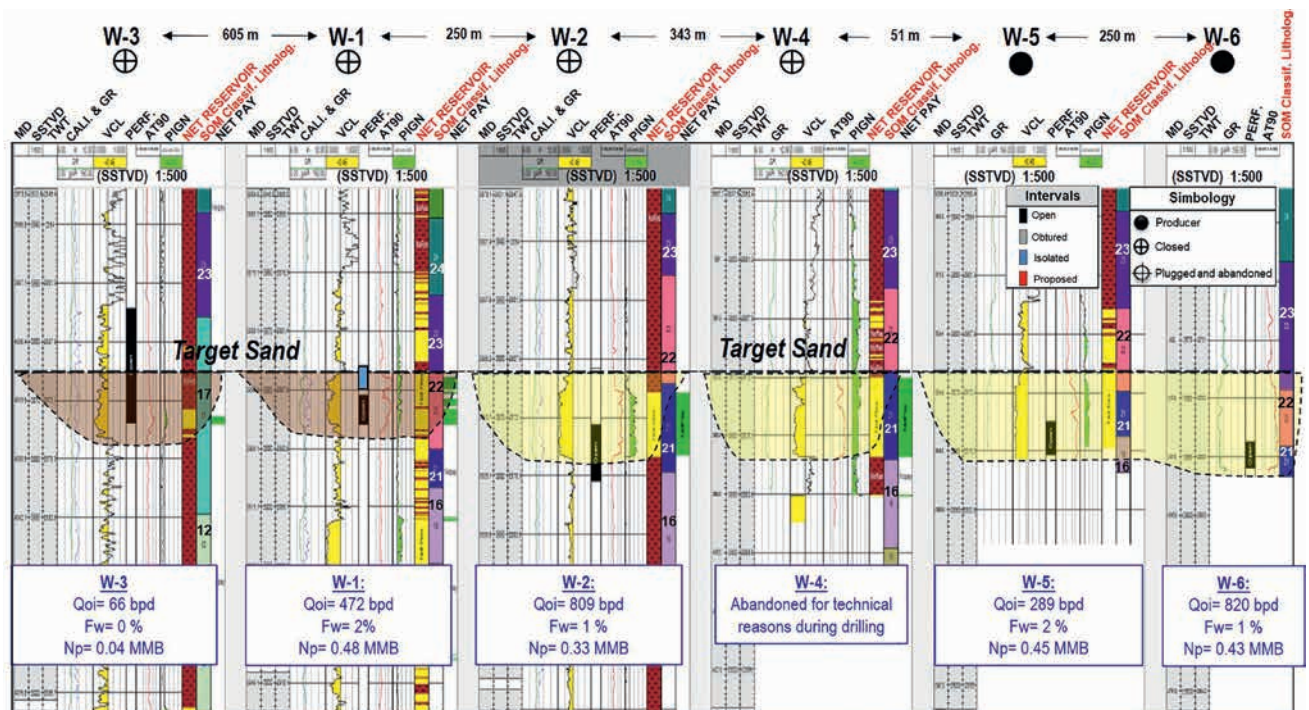


Figure 5 Stratigraphic section showing target sand and discrete tracks for Net Reservoir, Lithological Contrast SOM, and Net Pay.

The main objective of this statistical method is to identify how specific neurons are vertically concentrated along one or more logs. As an illustration of the technique, a diagram of the stratigraphic grid is shown in Figure 6. The VPC was extracted

from the whole 3D grid of SOM classification volume for Lithological Contrast, and detection was generated by counting the occurrence among the 25 neurons or classes in each stratigraphic layer in the VPC extracted from the grid. The VPC

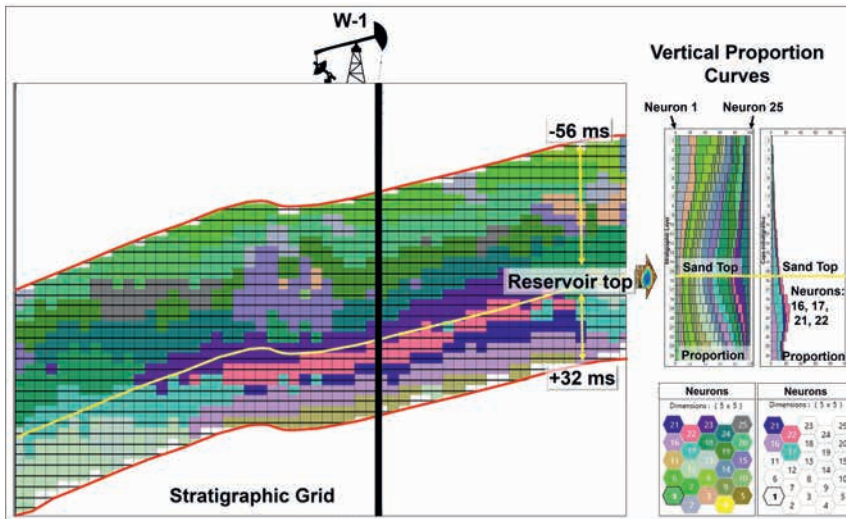


Figure 6 Vertical proportion Curve to identify neurons related to reservoir rock.

Neuron	Type	Net_Reservoir		Total
		No reservoir	Net reservoir	
N16	Count	34	43	77
	"% within Net_reservoir"	8,6%	7,8%	8,1%
	% of Total	3,6%	4,5%	8,1%
N17	Count	215	49	264
	"% within Net_reservoir"	54,2%	8,9%	27,9%
	% of Total	22,7%	5,2%	27,9%
N21	Count	39	258	297
	"% within Net_reservoir"	9,8%	47,0%	31,4%
	% of Total	4,1%	27,3%	31,4%
N22	Count	57	155	212
	"% within Net_reservoir"	14,4%	28,2%	22,4%
	% of Total	6,0%	16,4%	22,4%
N23	Count	52	44	96
	"% within Net_reservoir"	13,1%	8,0%	10,1%
	% of Total	5,5%	4,7%	10,1%
Total	Count	397	549	946
	% within Net_reservoir	100,0%	100,0%	100,0%
	% of Total	42,0%	58,0%	100,0%

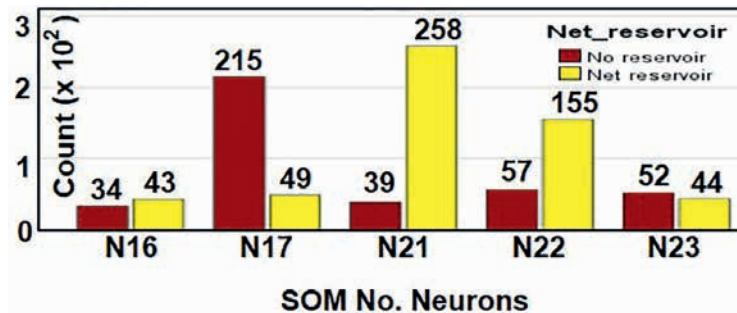


Table 2 Cross Tab for Lithological Contrast SOM versus net reservoir.

of SOM neurons exhibits remarkable slowly varying characteristics indicative of geologic depositional patterns. The reservoir top corresponds to stratigraphic layer No 16. In the VPC on the right, only neurons N16, N17, N21, and N22 are present. These neurons have a higher percentage occurrence relative to all 25 classes from the top of the target sand downwards. Corroborat-

ing the statistics, these same neural classes appear in the map view in Figure 3 and the vertical section shown in Figure 4. The stratigraphic well section in Figure 5 also supports the statistical results. It is important to note that these neurons also detected seismic samples above the the sand top, although of a lesser proportion. This effect is consistent with the existence of layers

with similar lithological characteristics, which can be seen from the well logs.

Bivariate statistical analysis cross tabs

The first step in this methodology is a bivariate analysis through cross-tabs (contingency table) to determine if two categorical variables are related based on observing the extent to which the occurrence of one variable is repeated in the categories of the second. Given that one variable is analysed in terms of another, a distinction must be made between dependent and independent variables. With cross tabs analysis, the possibilities are extended to (in addition to frequency analyses for each variable, separately) the analyses of the joint frequencies or those in which the analysis unit nature is defined by the combination of two variables.

The result was obtained by extracting the SOM classification volume along wells paths and constructing a discrete well log with two categories: ‘Net Reservoir’ and ‘not reservoir’. The distinction between ‘Net Reservoir’ and ‘not reservoir’ simply means that the dependent variable might have a hydrocarbon storage capacity or not. In this case, the dependent variable corresponds to neurons of SOM classification for Lithological Contrast volume. It is of ordinal type, since it has an established internal order, and the change from one category to another is not the same. The neurons go from N1 to N25, organized in rows. The independent variable is Net Reservoir, which is also an ordinal type variable. In this tab, the values organized in rows correspond to neurons from the SOM classification volume for Lithological Contrast, and in the columns are discrete states of the ‘Net Reservoir’ and ‘not reservoir’ count for each neuron. Table 2 shows that the highest Net Reservoir counts are associated with neurons N21 and N22 at 47.0% and 28.2% respectively. Conversely, lower counts of Net Reservoir are associated with neurons N17 (8.9%), N16 (7.8%) and N23 (8.0%).

Neuron N21 was detected at reservoir depth in wells W-2 (producer), W-4 (abandoned for technical reasons during drilling), W-5 (producer) and W-6 (producer). N21 showed higher percentages of occurrence in Net Reservoir, so this neuron could be identified as indicating the highest storage capacity. N22 was present in wells W-1 and W-6 at target sand depth but also detected in wells W-2, W-4 and W-5 in clay-sandy bodies

overlying the highest quality zone in the reservoir. N22 was also detected in the upper section of target sand horizontally navigated by the W-6 well, which has no petrophysical evaluation. N17 was only detected in well W-3, a minor producer of oil, which was sedimentologically cataloged as lobular facies and had the lowest reservoir rock quality. N16 was detected in a very small proportion in wells W-4 (abandoned for technical reasons during drilling) and W-5 (producer). Finally, N23 was only detected towards the top of the sand in well W-6, and in clayey layers overlying it in the other wells. This is consistent with the observed percentage of 8% Net Reservoir, as shown in Table 2.

Chi-Square independence hypothesis testing

After applying the cross-tab evaluation, this classified information was the basis of a Chi-Square goodness-of-fit test to assess the independence or determine the association between two categorical variables: Net Reservoir and SOM neurons. That is, it aims to highlight the absence of a relationship between the variables. The Chi-Square test compared the behaviour of the observed frequencies for each Lithological Contrast neuron with respect to the Net Reservoir variable (grouped in ‘Net Reservoir’ and ‘no reservoir’), and with the theoretically expected frequency distribution when the hypothesis is null.

As a starting point, the null hypothesis formulation was that the Lithological Contrast SOM neuron occurrences are independent of the presence of Net Reservoir. If the calculated Chi-Square value is equal to or greater than a certain critical theoretical value, the null hypothesis must be rejected. Consequently, the alternative hypothesis must be accepted. Observe the results in Table 3 where the calculated Chi-Square is greater than the theoretical critical value ($296 \geq 9.4$, with four degrees of freedom and 5% confidence level), so the null hypothesis of the independence of Net Pay with SOM neurons is rejected, leaving a relationship between Net Reservoir and Lithological Contrast SOM variables.

The test does not report a goodness of fit magnitude (substantial, moderate or poor), however. To measure the degree of correlation between both variables, Pearson’s Phi (φ) and Cramer’s V (v) measures were computed. Pearson’s φ coefficient was estimated from equation 1.1.

(Calculated)	Value	Degrees of freedom	Phi	Cramer’s V	No. Of Valid Cases							
Pearson Chi-Square	296,106	4	0,559	0,559	946							
Theoretical Chi-Square												
p = probability of having obtained a value less extreme than this point, v= degrees of freedom												
v/p	0,001	0,0025	0,05	0,01	0,025	0,05	0,1	0,15	0,2	0,25	0,3	0,35
1	10,8274	9,1404	7,8794	6,6349	5,0239	3,8415	2,7055	2,0722	1,6424	1,3233	1,0742	0,8735
2	13,8150	11,9827	10,5000	9,2104	7,3778	5,9915	4,6052	3,7942	3,2189	2,7726	2,4079	2,0996
3	16,2660	14,3202	12,8381	11,3449	9,3484	7,8147	6,2514	5,3170	4,6416	4,1083	3,6649	3,2831
4	18,4662	16,4238	14,8602	13,2767	11,1433	9,4877	7,7794	6,7449	5,9886	5,3853	4,8784	4,4377
5	20,5147	18,3854	16,7496	15,0863	12,8325	11,0705	9,2363	8,1152	7,2893	6,6257	6,0644	5,5731

Table 3 Calculated and theoretical Chi-Square values and its correlation measures.

$$\varphi = \sqrt{\frac{X^2}{n}} \tag{1}$$

Where X^2 : Chi-Square and n : No. of cases

Additionally, Cramer's V was estimated using equation. 1.2.

$$v = \frac{\varphi}{\min[(Rows - 1) * (Columns - 1)]} \tag{2}$$

In both cases, values near zero indicate a poor or weak relationship while values close to one indicate a strong relation. The authors obtained values for φ , and Cramer's v equals to 0.559 (Table 3). Based on this result, we can interpret a moderate relationship between both variables.

Box-and-Whisker plots

Box-and-whisker plots were constructed to compare and understand the behaviour of petrophysical properties for the range that each neuron intersects the well paths in the SOM volume. Also, these quantify which neurons of interest respond to Net Reservoir and Net Pay properties (Figure 7). Five descriptive measures are shown for a box-and-whisker plot of each property:

- Median (thick black horizontal line)
- First quartile (lower limit of the box)
- Third quartile (upper limit of the box)
- Maximum value (upper end of the whisker)
- Minimum value (lower end of the whisker)

The graphs provide information about data dispersion, i.e., the longer the box and whiskers, the greater the dispersion and also data symmetry. If the median is relatively centered in the box, the distribution is symmetrical. If, on the contrary, it approaches the first or third quartile, the distribution could be skewed to these quartiles, respectively. Finally, these graphs identify outlier observations that depart from the rest of the data in an unusual way (these are represented by dots and asterisks as less or more distant from the data centre). The horizontal dashed green line is the cut-off value for Effective Porosity (PIGN >0.10) while the dashed blue line represents the cut-off value for Clay Volume (VCL >0.45) and, dashed beige line is cut-off value for Water Saturation (SUWI <0.65).

Based on these data and the resulting analysis, it can be inferred that neurons N16, N17, N21, N22, and N23 respond positively to Net Reservoir. Of these neurons, the most valuable predictors are N21 and N22 since they present lower clay content in comparison with neurons N16 and N23 and associated

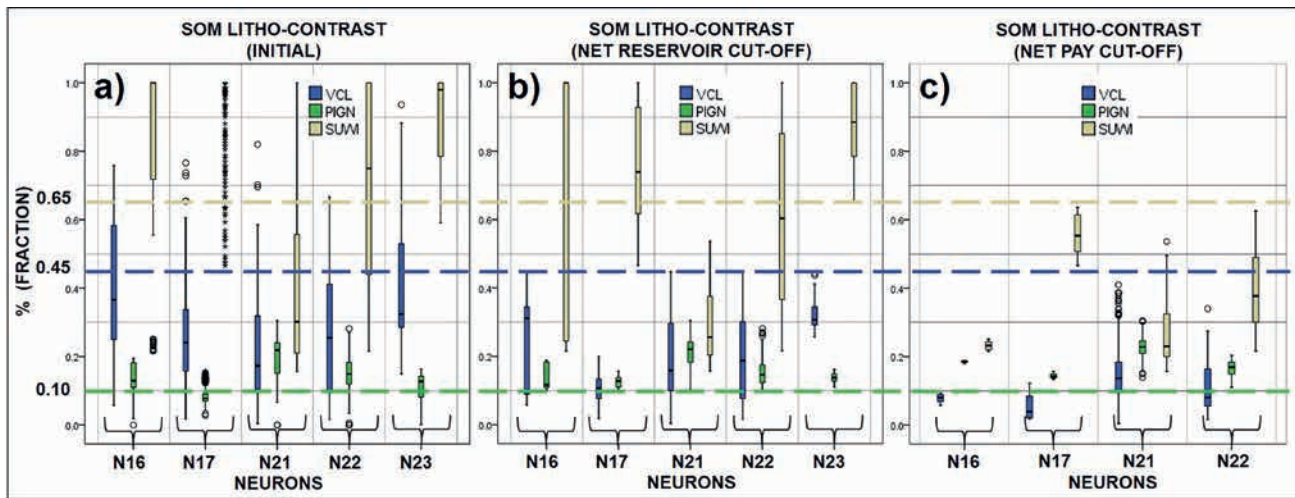


Figure 7 Comparison between neurons according to petrophysical properties: VCL (Clay Volume), PIGN (Effective Porosity) and SUWI (Water Saturation). a) SOM neurons for lithological contrast detection, b) Those that pass Net Reservoir cut-off and c) Those that pass Net Pay cut-off.

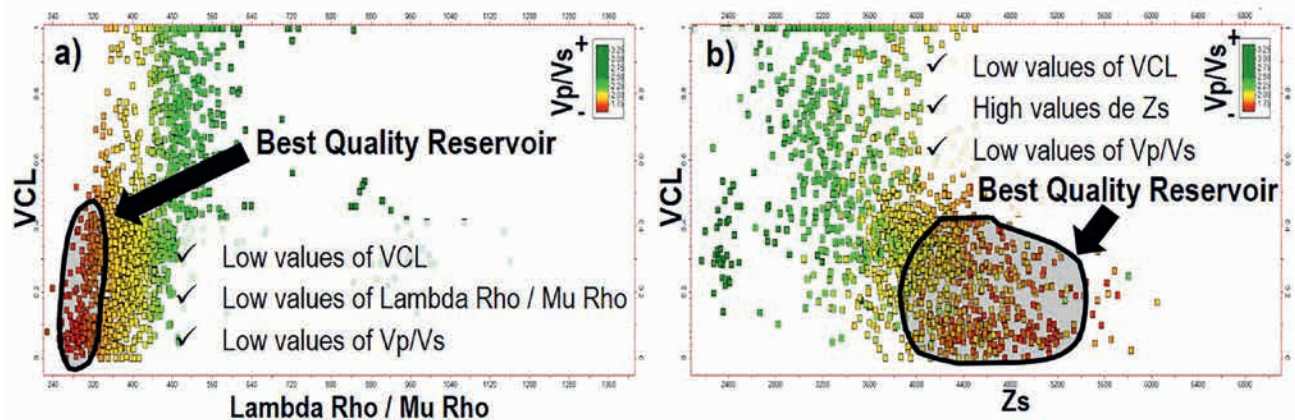


Figure 8 Scatter plots: a) Lambda Rho and Mu Rho ratio versus VCL and Vp/Vs y b) Zs versus VCL and Vp/Vs.

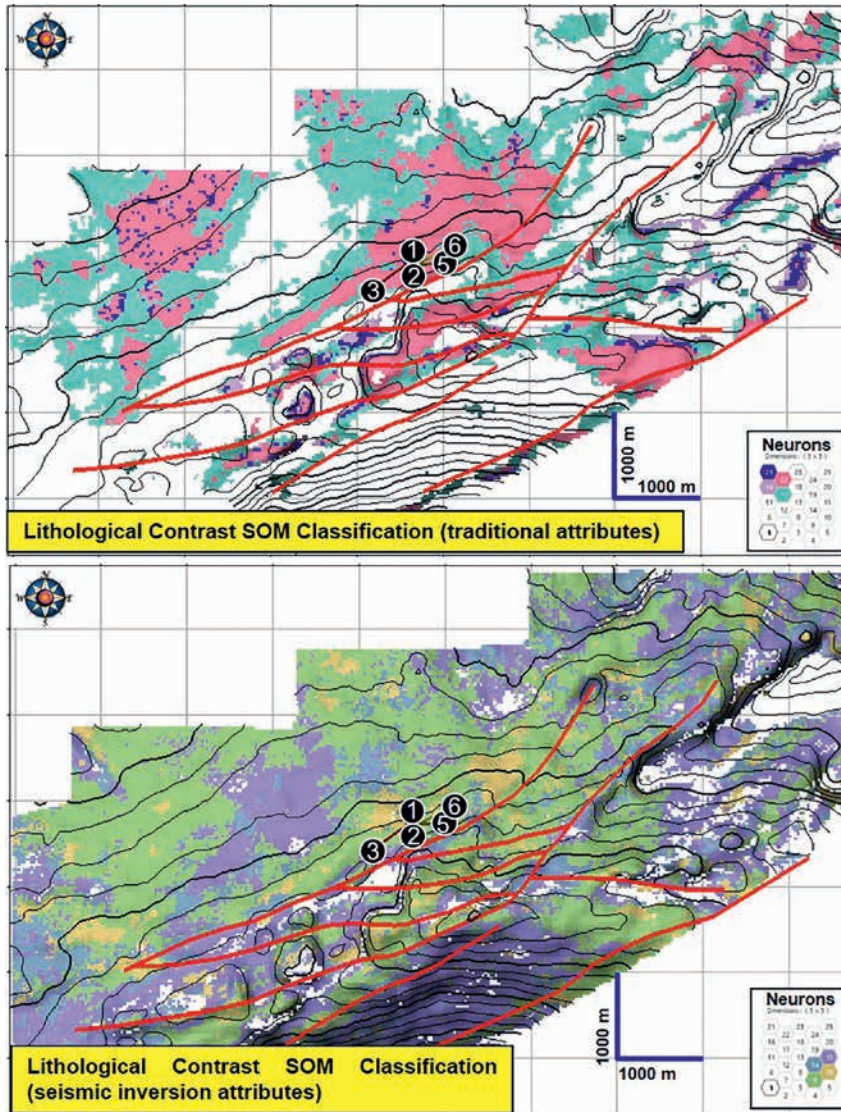


Figure 9 Plan view of neurons with geological meaning. Up: SOM Classification from traditional attributes. Down: SOM Classification from simultaneous inversion attributes.

higher Effective Porosity shown by neurons N16, N17, and N23 (Figure 7a). Neurons N21 and N22 are ascertained to represent the best reservoir rock quality. Finally, neuron N23 (Figure 7b) can be associated with rock lending itself to storage capacity, but clayey and with high water saturation, which allows it to be discarded as a significant neuron. It is important to note that this analysis was conducted by accounting for the simultaneous occurrence of the petrophysical values (VCL, PIGN, and SUWI) on the neurons initially intersected (Figure 7a), and then on the portion of the neurons that pass Net Reservoir cut-off values (Figure 7b), and finally on the portion of the neurons that pass net-pay cut-off values (Figure 7c). For all these petrophysical reasons, the neurons to be considered as a reference to estimate the lateral and vertical distribution of Net Reservoir associated with the target sand are in order of importance, N21, N22, N16, and N17.

Simultaneous seismic inversion

During this study, a simultaneous prestack inversion was performed using 3D seismic data and sonic logs, in order to estimate seismic petrophysical attributes as Acoustic Impedance (Z_p), Shear Impedance (Z_s), Density (ρ), as well as P&S-wave

velocities, among others. They are commonly used as lithology indicators, possible fluids, and geomechanical properties. Figure 8a shows a scatter plot from well data of seismic attributes Lambda Rho and Mu Rho ratio versus Clay Volume (VCL) and as a discriminator V_p/V_s ratio (V_p/V_s). The target sand corresponds to low V_p/V_s and Lambda/Mu values (circled in the figure). Another discriminator in the reservoir was S-wave impedance (Z_s) (Figure 8b). From this, seismic inversion attributes were selected for classification by SOM neural network analysis. These attributes were V_p/V_s ratio, Lambda Rho/Mu Rho ratio, and Z_s .

Self-organizing map (SOM) comparison

Figure 9 is a plan view of neuron-extracted geobodies associated with the sand reservoir. In the upper part, a SOM classification for Lithological Contrast detection obtained from six traditional seismic attributes is shown, and in the lower part, a different SOM classification for Lithological Contrast detection was obtained from three attributes of simultaneous inversion. Both results are very similar. The selection of SOM classification neurons from inversion attributes was done through spatial pattern recognition, i.e., identifying geometry/shape of the clusters

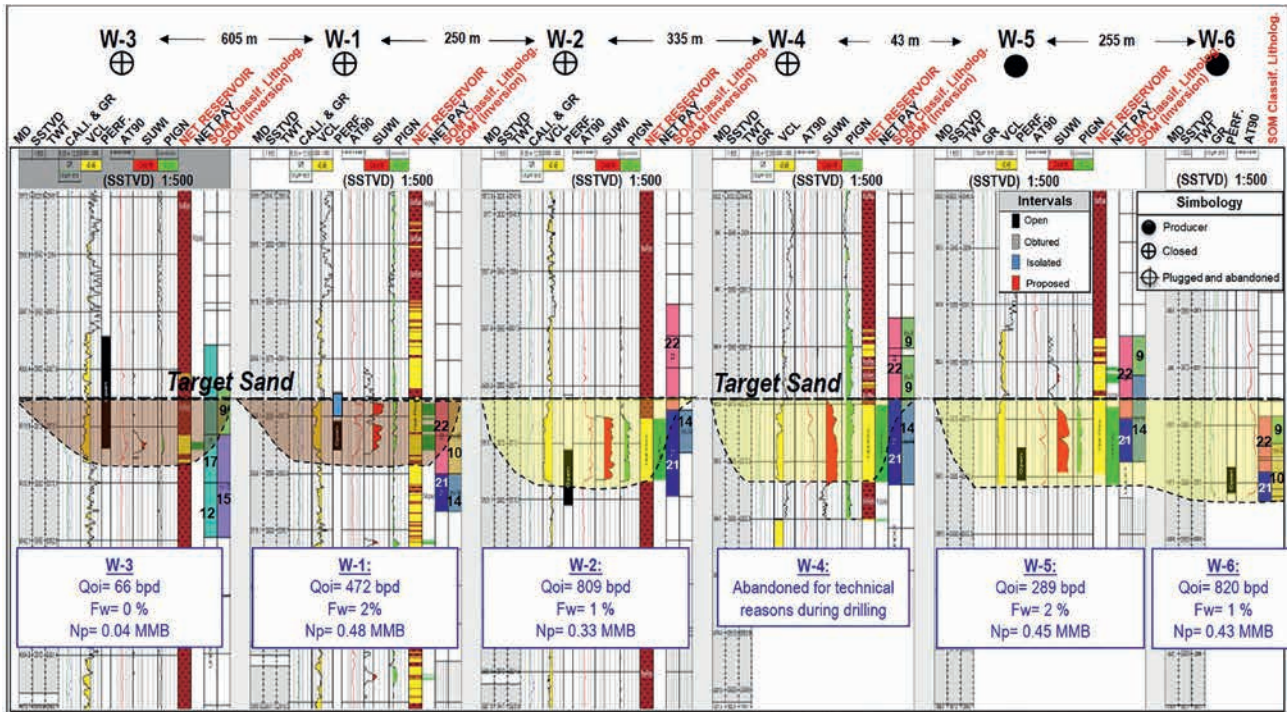


Figure 10 Well stratigraphic section showing the target zone with tracks for discrete logs from Net Reservoir, Net Pay and both SOM classifications.

related to each of 25 neurons congruent with the sedimentary model, and by using a stratigraphic section for wells that includes both SOM classifications tracks.

Figure 10 shows a well stratigraphic section that includes a track for Net Reservoir and Net Pay classification along with SOM classifications from traditional attributes and a second SOM from simultaneous inversion attributes defined from SOM volumes and well paths intersection. In fact, only the neurons numbers with geological meaning are shown.

Discussion and conclusions

Principal Component Analysis (PCA) identified the most significant seismic attributes to be classified by Self-Organizing Maps (SOM) neural network at a single-sample basis to detect features associated with lithological contrast and recognize lateral and vertical extension in the reservoir. The interpretation of SOM classification volumes was supported by multidisciplinary sources (geological, petrophysical, and dynamic data). In this way, the clusters detected by certain neurons became the inputs for geobody interpretation. The statistical analysis and visualization techniques enabled the estimation of Net Reservoir for each neuron. Finally, the extension of reservoir rock geobodies derived from SOM classification of traditional attributes was corroborated by the SOM acting on simultaneous inversion attributes. Both multi-attribute machine learning analysis of traditional attributes seismic inversion attributes enable refinement of the sedimentary model to reveal more precisely the lateral and vertical distribution of facies. However, the Lithological Contrast SOM results from traditional attributes showed a better level of detail compared with seismic inversion SOM.

Collectively, the workflow may reduce uncertainty in proposing new drilling locations. Additionally, this methodology might be applied using specific attributes to identify faults and fracture zones, identify absorption phenomena, porosity changes, and direct hydrocarbon indicator features, and determine reservoir characteristics.

Acknowledgments

The authors would like to thank Pemex and Oil and Gas Optimization for providing software and technical resources. Thanks also are extended to Geophysical Insights for the research and development of the Paradise® AI workbench and the machine learning applications used in this paper. Finally, we would like to thank Reinaldo Michelena, María Jerónimo, Tom Smith, and Hal Green for review of the manuscript.

References

Agresti, A. [2002]. *Categorical Data Analysis*. John Wiley & Sons.
 Kohonen, T. [1982]. Self-organized formation of topologically correct feature maps. *Biological Cybernetics*, **43**, 59-69.
 Kohonen, T. [2001]. *Self-Organizing Maps*. Third, Extended Edition. Springer Series in Information Sciences vol. 30, Springer-Verlag, Berlin, Germany. Marroquín I., Brault, J.J. and Hart, B. [2009]. A visual data mining methodology to conduct seismic facies analysis: Part 2 - Application to 3D seismic data. *Geophysics*, **1**, 13-23.
 Roden R., Smith, T. and Sacrey, D. [2015]. Geologic pattern recognition from seismic attributes: Principal component analysis and self-organizing maps. *Interpretation*, **4**, 59-83.
 Vilorio R. and Taheri, M. [2002]. Metodología para la Integración de la Interpretación Sedimentológica en el Modelaje Estocástico de Facies Sedimentarias, (INT-ID-9973, 2002). *Technical Report*, INTEVEP-PDVSA.